

Article

Influence of Site-Dependent Pigment-Protein Interactions on Excitation Energy Transfer in Photosynthetic Light Harvesting

Eva Rivera, Daniel Montemayor, Marco Masia, and David Coker

J. Phys. Chem. B, **Just Accepted Manuscript** • DOI: 10.1021/jp4011586 • Publication Date (Web): 18 Apr 2013

Downloaded from <http://pubs.acs.org> on April 29, 2013

Just Accepted

"Just Accepted" manuscripts have been peer-reviewed and accepted for publication. They are posted online prior to technical editing, formatting for publication and author proofing. The American Chemical Society provides "Just Accepted" as a free service to the research community to expedite the dissemination of scientific material as soon as possible after acceptance. "Just Accepted" manuscripts appear in full in PDF format accompanied by an HTML abstract. "Just Accepted" manuscripts have been fully peer reviewed, but should not be considered the official version of record. They are accessible to all readers and citable by the Digital Object Identifier (DOI®). "Just Accepted" is an optional service offered to authors. Therefore, the "Just Accepted" Web site may not include all articles that will be published in the journal. After a manuscript is technically edited and formatted, it will be removed from the "Just Accepted" Web site and published as an ASAP article. Note that technical editing may introduce minor changes to the manuscript text and/or graphics which could affect content, and all legal disclaimers and ethical guidelines that apply to the journal pertain. ACS cannot be held responsible for errors or consequences arising from the use of information contained in these "Just Accepted" manuscripts.



ACS Publications
High quality. High impact.

The Journal of Physical Chemistry B is published by the American Chemical Society.
1155 Sixteenth Street N.W., Washington, DC 20036
Published by American Chemical Society. Copyright © American Chemical Society.
However, no copyright claim is made to original U.S. Government works, or works
produced by employees of any Commonwealth realm Crown government in the course
of their duties.

Influence of Site-Dependent Pigment-Protein Interactions on Excitation Energy Transfer in Photosynthetic Light Harvesting

Eva Rivera,[†] Daniel Montemayor,[†] Marco Masia,^{‡,§} and David F. Coker^{*,¶,||}

Department of Physics, and Complex Adaptive Systems Laboratory, University College Dublin, Belfield, Dublin 4, Ireland, Institut für Physikalische und Theoretische Chemie, Goethe Universität Frankfurt Max von Laue Str. 7, D-60438 Frankfurt am Main, Germany and Dipartimento di Chimica e Farmacia, Università degli Studi di Sassari, Via Vienna 2, 07100 Sassari, Italy, and Department of Chemistry, Boston University, 590 Commonwealth Avenue, Boston, MA 02215, USA

E-mail: coker@bu.edu

[†]University College Dublin

[‡]Goethe Universität Frankfurt and Università degli Studi di Sassari

[¶]Boston University

[§]Current address: Department of Chemistry, Boston University, 590 Commonwealth Avenue, Boston, MA 02215, USA

^{||}Also at: Department of Physics, and Complex Adaptive Systems Laboratory, University College Dublin, Belfield, Dublin 4, Ireland

Abstract

A site dependent spectral density system-bath model of the Fenna-Matthews-Olsen (FMO) pigment-protein complex is developed using results from ground state molecular mechanics simulations together with a partial charge difference model for how the long-range contributions to the chromophore excitation energies fluctuate with environmental configuration. A discussion of how best to consistently process the chromophore excitation energy fluctuation correlation functions calculated in these classical simulations to obtain reliable site-dependent spectral densities is presented. The calculations reveal that chromophores that are close to the protein-water interface can experience strongly dissipative environmental interactions characterized by solvent reorganization energies that can be as much as two - three times those of chromophores that are buried deep in the hydrophobic protein scaffolding. Using a linearized density matrix quantum propagation method we demonstrate that the inhomogeneous system-bath model obtained from our site-dependent spectral density calculations give results consistent with experimental dissipation and dephasing rates. Moreover, we show that this model can simultaneously enhance the energy transfer rate and extend the decoherence time. Finally, we explore the influence of initially exciting different chromophores and mutating local environments on energy transfer through the network. These studies suggest that different pathways, selected by varying initial photoexcitation, can exhibit significantly different relaxation times depending on whether the energy transfer path involves chromophores at the protein-solvent interface or if all chromophores in the pathway are buried in the protein.

Keywords: Coherent Excitation Energy Transfer, Photosynthetic Light Harvesting, Dissipative Quantum Dynamics, Spectral Density, Environmental Effects

Introduction

Most models of dissipative energy transfer in protein-pigment complexes assume that the local environment of each chromophore in these biological light harvesting energy transmission networks are identical despite the often significant local differences in protein structure around each chromophore. In this paper we employ classical molecular mechanics simulation methods and a model of how chromophore excitation energies depend on their surroundings to compute chromophore dependent spectral densities and explore how local differences in environmental fluctuations determined by these quantities influence energy transfer processes in these systems. We employ the well characterized and widely studied Fenna-Matthews-Olsen (FMO) “excitonic wire” protein-pigment complex as a benchmark system to show that realistic models of the chromophore-environmental interactions display heterogeneous dissipation characteristics from the different chromophore sites in such networks. Thus, for example, our studies reveal that chromophores buried deep in the protein generally show slower dissipation and dephasing due to weaker environmental coupling, while chromophores at the protein-solvent interface show more rapid relaxation due to stronger interactions with solvating water molecules. The role of different chromophore coordinating protein components (side chains and backbone) is explored and our studies suggest that local variation in such coordination could offer a general way to tune and control the energy transport properties of these networks. Our model dissipative quantum dynamical studies indicate that such differences in local environmental characteristics can significantly influence energy transport in these systems.

Multidimensional nonlinear spectroscopic experiments¹⁻⁴ have demonstrated that the early stages of photo-excitation and excitation energy transfer in various photosynthetic light harvesting complexes involve relatively long lived coherent quantum dynamics in which the energy moves through these quantum networks via processes that are characterized by a balance of coherent beating of the amplitudes of the different excited chromophore states and dissipative relaxation from higher to lower energy states. Remarkably, the spectroscopic signatures of coherent excitation energy transfer dynamics, observed as oscillatory beating features in nonlinear optical signals that are related to the electronic coherence in these systems, are even found at ambient temperatures^{1,2}

where such quantum coherent behavior is usually expected to be damped out.

Biological light harvesting systems generally involve assemblies of chromophores arrayed in structured complexes embedded in a protein scaffolding as displayed for the FMO system in the panels of Figure 1. The different chromophores in these structures generally show a diversity of local protein environments. The FMO system, for example, has Bacterio Chlorophyll (BChl) chromophores that are buried deep in the protein of the individual monomer structural units such as BChl7 (displayed as the orange-gold chromophore in the figure). There are also chromophores that play critical roles in the inter-connectivity of the different parts of these energy transfer networks that can be more loosely bound, and near the surface of the protein complexes. Chromophore BChl8 (the grey chromophore) in the *in vivo* assembled FMO trimer complex, for example, is located at the interface between the different monomers and is highly labile and its properties may be significantly influenced by the water solvent environment.⁵⁻⁸

The studies reported here employ realistic molecular mechanics models of the fluctuations in the local environment and how they influence dynamical fluctuations in the individual chromophore excitation energies.

Reliable modeling of the short time coherent excitation energy transfer and long time thermal equilibration in these light harvesting chromophore networks presents a significant challenge to conventional theoretical approaches such as Förster resonance energy transfer (FRET) theory,^{9,10} or employing the Redfield^{11,12} or Lindblad equations,^{13,14} which can in some situations, provide inaccurate descriptions of these processes due to various approximations employed (e.g. use of perturbation theory,¹⁵ the incoherent transfer approximation,⁹ the markovian approximation,¹⁵⁻¹⁷ the secular approximation,^{13,16,17} or high temperature approximations) that can limit their applicability when treating realistically parameterized models of light harvesting complexes.

The limitations of many of these approximations and the shortcomings for the particular application to photosynthetic light harvesting networks have been discussed elsewhere.¹⁶ To overcome these limitations of the conventional methods within this context, various efforts have been made by a number of authors.⁹⁻²⁴ Recently we developed a new approach^{25,26} for implementing the

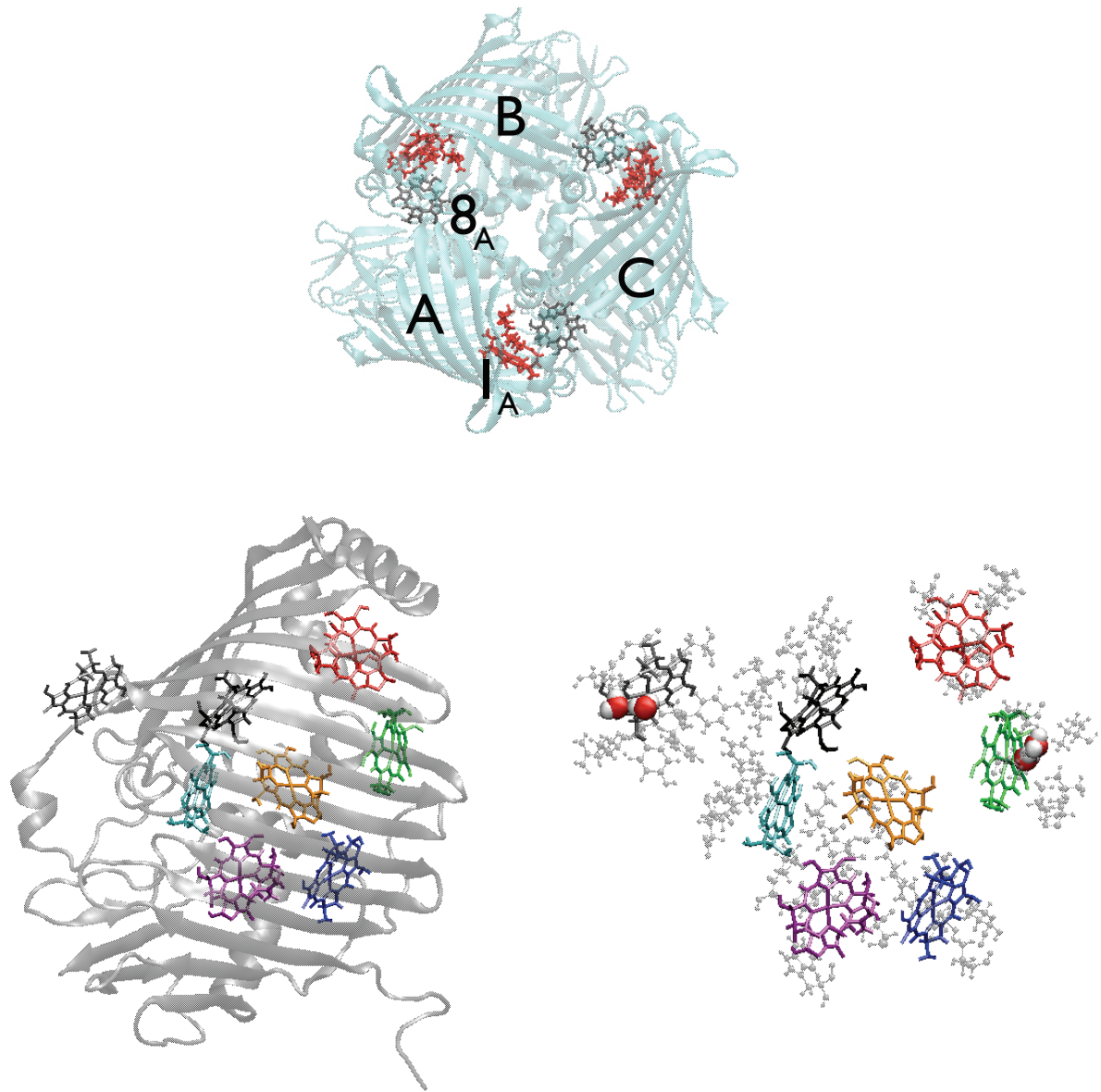


Figure 1: Bottom left panel: Structure of the FMO pigment-protein monomer complex showing the eight Bacterio Chlorophyll (BChl) porphyrin rings embedded in the protein backbone ribbon structure. Rings are colored coded to match presentation of other results throughout the paper (BChl1:red, BChl2:green, BChl3:blue, BChl4:magenta, BChl5:cyan, BChl6:black, BChl7:gold, BChl8:grey). Bottom right panel: Detailed local structure showing coordinating side chains and groups within a radius of 10 Å of the center of each BChl porphyrin. Top panel: Assembly of monomer units to form FMO trimer - the structure that is found *in vivo*. Relative packing of the monomers within the trimer places BChl8 from monomer A adjacent to BChl1 from monomer B, *etc.*

linearized density matrix propagator^{27–31} that shows considerable promise for reliably extending these ideas to treat significantly longer time dynamics in complex systems, such as photosynthetic light harvesting networks.³² This new partial linearized density matrix (PLDM) propagation approach overcomes many of the sampling problems associated with averaging phase factor trajectory weights encountered when applying such methods for long times. This PLDM propagation approach is used below to explore the influence of different system-bath interaction models on the quantum dynamics of energy transfer in the heterogenous environments.

Model Calculations

The model hamiltonian used here to describe the FMO light harvesting complex has a quantum subsystem component, \hat{H}_S , that contains only system operators, a bath operator term \hat{H}_B , and the system-bath coupling term, \hat{H}_{SB} that contains both system and bath quantities. In this model of the system-bath coupling terms each chromophore experiences dissipative interactions with its own independent bath, thus the general model hamiltonian has the following form:

$$\begin{aligned} \hat{H} = \hat{H}_S + \hat{H}_{SB} + \hat{H}_B = & \sum_{\alpha=1}^{N_{state}} \left\{ \epsilon_{\alpha} + \sum_{l=1}^{n^{(\alpha)}} c_l^{(\alpha)} \hat{x}_l^{(\alpha)} + \sum_{\beta=1}^{N_{state}} \sum_{m=1}^{n^{(\beta)}} \frac{1}{2} \left[\hat{p}_m^{(\beta)2} + \omega_m^{(\beta)2} \hat{x}_m^{(\beta)2} \right] \right\} |\alpha\rangle\langle\alpha| \\ & + \sum_{\alpha < \beta}^{N_{state}} \Delta_{\alpha,\beta} [|\alpha\rangle\langle\beta| + |\beta\rangle\langle\alpha|] \end{aligned} \quad (1)$$

The electronic hamiltonian,¹⁸ \hat{H}_S , is determined by the diagonal electronic site excitation energies, ϵ_{α} , of the chromophores, and the off-diagonal electronic couplings between the chromophores, $\Delta_{\alpha,\beta}$. The full set of parameters defining \hat{H}_S , together with various computed system-bath interaction quantities are summarized schematically in Figure 2.

The spectral densities,³³ $j^{(\alpha)}(\omega)$, that determine the chromophore dependent system-bath cou-

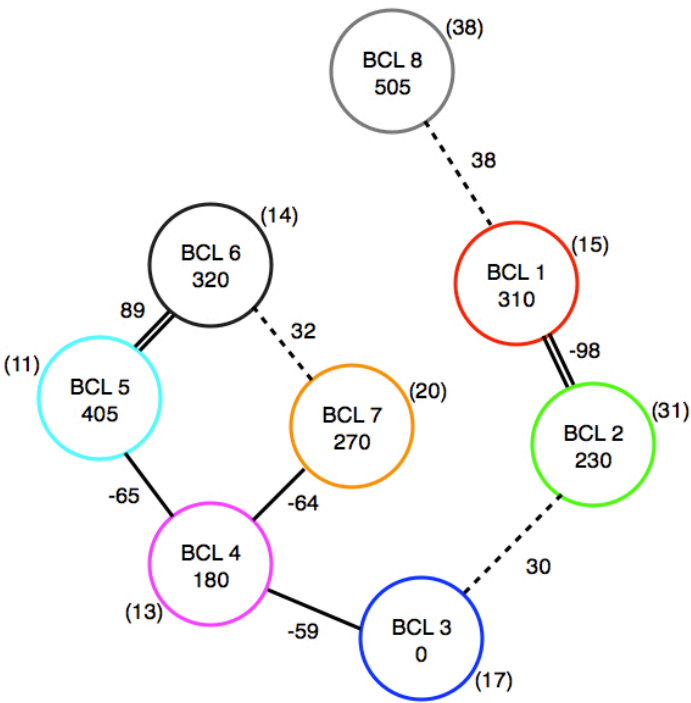


Figure 2: Schematic of eight chromophore model FMO hamiltonian (all values in cm^{-1}). Each color coded circle represents a BChl chromophore labeled by its relative site excitation energy, ϵ_{α} . Electronic couplings $\Delta_{\alpha,\beta}$, label connections (strong-double, medium-single, weak-dashed). Values in parentheses give local solvent reorganization energies, λ_{α} .

Eva Rivera et al.

Influence of Site-Dependent Pigment- ...

pling strengths, $c_l^{(\alpha)}$, according to

$$j^{(\alpha)}(\omega) = (\pi/2) \sum_l^{n^{(\alpha)}} (c_l^{(\alpha)2} / \omega_l^{(\alpha)}) \delta(\omega - \omega_l^{(\alpha)}) \quad (2)$$

are obtained as follows: For the model hamiltonian presented in Eq.(1), the excitation energy of chromophore α fluctuates as a linear function of the bi-linearly coupled harmonic bath coordinates associated with this chromophore as described by the term $\delta\hat{\epsilon}_\alpha(t) = \sum_l^{n^{(\alpha)}} c_l^{(\alpha)} \hat{x}_l^{(\alpha)}(t)$. We define the excitation energy fluctuation correlation function of chromophore α as

$$\mathcal{C}_\alpha(t) = \langle \delta\hat{\epsilon}_\alpha(0) \delta\hat{\epsilon}_\alpha(t) \rangle = \sum_l^{n^{(\alpha)}} c_l^{(\alpha)2} \langle \hat{x}_l^{(\alpha)}(0) \hat{x}_l^{(\alpha)}(t) \rangle \quad (3)$$

where the angle brackets represent an equilibrium ensemble average over the thermal distribution of the states of this harmonic bath. If the independent chromophore baths are described classically we find that $\langle \hat{x}_l^{(\alpha)}(0) \hat{x}_l^{(\alpha)}(t) \rangle_{cl} = \cos \omega_l^{(\alpha)} t / \beta \omega_l^{(\alpha)2}$. Alternatively,³⁴ for a quantum description of the harmonic bath we obtain $\langle \hat{x}_l^{(\alpha)}(0) \hat{x}_l^{(\alpha)}(t) \rangle_{qu} = [\coth(\beta \hbar \omega_l^{(\alpha)} / 2) \cos \omega_l^{(\alpha)} t - i \sin \omega_l^{(\alpha)} t] \hbar / 2 \omega_l^{(\alpha)}$. Thus the excitation energy fluctuation correlation functions for the classical and quantum baths are obtained as

$$\mathcal{C}_\alpha^{cl}(t) = (1/\beta) \sum_l^{n^{(\alpha)}} (c_l^{(\alpha)} / \omega_l^{(\alpha)})^2 \cos \omega_l^{(\alpha)} t \quad (4)$$

and

$$\mathcal{C}_\alpha^{qu}(t) = (\hbar/2) \sum_l^{n^{(\alpha)}} (c_l^{(\alpha)2} / \omega_l^{(\alpha)}) [\coth(\beta \hbar \omega_l^{(\alpha)} / 2) \cos \omega_l^{(\alpha)} t - i \sin \omega_l^{(\alpha)} t] \quad (5)$$

respectively. The cosine transforms of the real parts of these correlation function results can be straightforwardly manipulated to give different ways of processing these classical and quantum correlation functions to obtain the spectral density expression given above. Thus, using the fact that $\int_{-\infty}^{\infty} \exp(i\omega t) dt = 2\pi \delta(\omega)$, we find that

$$\beta \omega \int_0^\infty dt \mathcal{C}^{cl}(t) \cos \omega t = J^{cl}(\omega) \quad (6)$$

and

$$(2/\hbar) \tanh(\beta \hbar \omega / 2) \int_0^\infty dt \operatorname{Re}[\mathcal{C}^{qu}(t)] \cos \omega t = J^{qu}(\omega) \quad (7)$$

There is a long tradition of processing classical correlation functions by pretending that they are the same as the real part of the quantum correlation function and substituting them into Eq.(7). Using the expressions derived above it is easy to show that this procedure of processing the classical correlation function using the quantum result for extracting the spectral density will give a mixed, or “chimera” - like spectral density that is related to the true spectral density as follows

$$J^{mix}(\omega) = (2/\beta \hbar \omega) \tanh(\beta \hbar \omega / 2) J(\omega) \quad (8)$$

Clearly this mixed estimate of the spectral density has a significant unphysical temperature dependence as the true spectral density, being a property of the full system hamiltonian, should be completely independent of temperature. These different ways of processing correlation function results to obtain spectral densities are explored below and in the Supporting Information.

Since in general quantum correlation functions are very difficult to compute for large complex systems, the approach we adopt here is to compute classical equilibrium correlation functions of the excitation energy fluctuations of the various chromophores embedded in their local protein environments using a realistic classical molecular mechanics model of the solvated FMO trimer system. We then process these independent chromophore excitation energy fluctuation correlation functions according to Eq.(6) so that the classical simulation used to parameterize the environmental interactions and the system-bath model are consistent.

Our spectral density calculations thus proceed by first constructing and equilibrating a ground state molecular mechanics model of the FMO trimer in aqueous solution. The simulation details of these classical calculations are presented in the Supporting Information. Next we must compute the approximate excitation energies of the different chromophores in snapshot configurations along the equilibrium molecular dynamics trajectory that samples the classical fluctuations of the local protein environment around the different chromophores. Details of our calculations and a study of

the statistical convergence of the averaging of our spectral densities are presented in the Supporting Information.

There have been a number of recent computations of spectral densities based on similar philosophies to the approach we employ here.^{35–46} In addition to the differences in correlation function processing methodology outlined above, we also adopt a critically different approach for approximately computing the chromophore excitation energy fluctuations that result from the dynamics of the different local protein environments. We use the approach detailed and tested by Shi and coworkers⁴⁰ that is based on an idea originally presented by Renger and his collaborators.³⁹

There are two key problems with simply using *ab initio* electronic structure methods to compute the excitation energies along a trajectory of supposedly representative nuclear configurations obtained from classical MD simulations using a model ground state molecular mechanics (MM) force field:⁴⁷ (1) The effective model ground state (GS) MM potential surface employed in the MD simulations to generate the configurations may differ significantly from the *ab initio* ground state surface that forms the lower state in the electronic structure calculations of the excitation energy. Thus, for example, the minimum of the MM potential, about which the MD trajectory fluctuates, may be displaced from the minimum of the *ab initio* GS surface. This may be particularly problematic for higher frequency vibrations in which the effects of anharmonicities or small shifts in equilibrium bond lengths between the ground and excited state potentials may lead to significant over estimation of the magnitude of the fluctuations of the excitation energy gap. This may occur if the minimum of the MM surface is shifted from where it should be and causes the classical MD simulations to focus on unphysical regions of the *ab initio* ground and excited state surfaces, say on the steep repulsive walls where small differences can cause large changes in relative state energies. (2) Another problem that may also lead to an over-estimation of the magnitude of the excitation energy fluctuations using the combined MD - *ab initio* approach arises since this method approximates the excitation energy as the difference between the ground and excited state adiabatic potential energy surfaces. In this way the approach ignores the dispersion arising from the nuclear vibrational wave function that makes many different nuclear configurations sampled from

Eva Rivera et al.

Influence of Site-Dependent Pigment- ...

the same vibrational state wave function have the same total energy. Thus the estimate of excitation energy based on the difference in *ab initio* adiabatic surfaces neglects the quantum averaging over the nuclear vibrational state distribution. This problem, again, should be most severe for higher frequency vibrations where the potential surfaces vary more rapidly with nuclear coordinates.

A simple but effective way to approximately solve both these problems that are expected to most significantly influence the contributions from the higher frequency vibrations of the chromophores themselves is to use a similar procedure traditionally employed in simulations treating systems involving high frequency quantum vibrations in the presence of low frequency collective motions. In such simulations it is often useful to extract information about the large amplitude low frequency motions by freezing the small amplitude high frequency quantum modes at some mean representative geometry thus removing the spurious high frequency fluctuations that result from classical treatment of these high frequency motions. In this way inaccurately represented high frequency chromophore vibrations that can artificially dominate the excitation energy fluctuation correlation function signals can be effectively filtered out, enhancing the more reliable low frequency response that promotes dissipation by coupling to low energy coupled chromophore excitations. The long-range Coulomb interactions responsible for the low frequency dissipation in this network of chromophores with fairly closely spaced excitation energies are usually reliably treated as an external field associated with the partial charges in the molecular mechanics protein environment. The *ab initio* calculations typically fragment the system into a minimal chromophore piece that is treated quantum mechanically, in the presence of a long range Coulomb partial charge external field. In contrast, the approach that we have adapted here assumes that the different interactions between the ground and excited state charge distributions of the chromophores, for the purpose of computing the low frequency, long range part of the excitation energy fluctuations, can be represented by difference partial charges $\Delta q_i = (q_i^e - q_i^g)$ at the various charge sites, i , of the chromophores. The model uses ground and excited state point charges, q_i^g and q_i^e respectively, obtained from ground state minimum energy geometry gas phase calculations of the BChl chromophore using DFT with the B3LPY functional and these charge distributions have been fitted to

the point charge model as detailed in reference.³⁹ In these calculations the difference charge distribution of the chromophores is thus assumed to be identical for each chromophore and the unique excitation energy gap fluctuations of a given chromophore arise from fluctuations in its individual long range partial charge solvation environment. Thus the instantaneous excitation energy gap of chromophore α at time t is computed according to the following result:

$$\delta\epsilon_{\alpha}(t) = \frac{1}{4\pi\epsilon_0} \sum_i \sum_K \Delta q_i Q_K^{(\alpha)} / |r_i^{(\alpha)}(t) - R_K^{(\alpha)}(t)| \quad (9)$$

where the sum on i extends over difference partial charge sites located at positions $r_i^{(\alpha)}$ for chromophore α , and the sum on K extends over the partial charges, $Q_K^{(\alpha)}$, located at $R_K^{(\alpha)}$ in the environment of chromophore α .

The reduced system - bath model hamiltonian is amenable to open quantum system dissipative dynamical simulation using the partial linearized density matrix (PLDM) propagation scheme that our group has detailed and benchmarked in previous work.^{25,26,30} In the following we demonstrate that the quantum dynamics of these model systems is sensitive to the details of the differences in local dissipative environment around the various chromophores in the solvated FMO trimer pigment-protein complex as represented by the chromophore dependent system-bath model outlined here.

Results and Discussion

The typical snapshot configuration from our GS MD simulations displayed in the bottom right panel of Figure 1 reveals that the local environments around the various chromophores in the FMO trimer complex are, on average, significantly structurally different from one another and that for some chromophores, the surroundings can be quite static, but for others there can be considerable dynamical fluctuation. We see that chromophores BChl2 and BChl8, for example, are in regions of the protein that are open to the solvent and that typically a hydrogen-bonded pair of water

molecules can be found in the nearest 10 Å sphere of neighbors around these chromophores. In fact, from the left panel of Figure 3, where we display example configurations of the dominant coordination geometries of the Mg centers of all eight distinct bacteriochlorophylls sampled in our MD calculations on the solvated FMO trimer, we find that the Mg center of BChl2 is almost always coordinated by a water molecule that penetrates the local protein environment. For BChl8, on the other hand, there is always water present in the coordination sphere but BChl8's central Mg atom is often coordinated by a carbonyl (CO) group of the protein backbone. Chromophore BChl5 is also coordinated by a backbone CO group but it is buried deep within the hydrophobic regions of the protein. All other central Mg atoms of BChls 1, 3, 4, 6, and 7 are found to be coordinated by N-atoms of histidine side chains, though the coordinating histidine of BChl7 has a less well defined coordination geometry than the others.

The right panel of Figure 3 displays the spectral densities computed from the site excitation energy fluctuation correlation functions defined in Eq.(3). For the results presented here the site excitation energies are computed using the excitation partial charge difference result given in Eq.(9) and we have processed these correlation functions classically according to Eq.(6). We see that the spectral densities computed in this way both at T=77K and at T=300K agree well with one another. In the Supporting Information we present results obtained by taking our classical correlation functions and processing them according to the quantum result of Eq.(7) and we thus demonstrate that this inconsistent, mixed treatment yields unphysical temperature dependent results.³⁵

The detailed spectral densities presented in the right panel of Figure 3 show significant differences from site to site that correlate with structural differences in the local environments of the various BChl chromophores. The parenthetical values in Figure 2 summarize the solvent reorganization energies, $\lambda_{\alpha} = \frac{1}{\pi} \int d\omega j^{(\alpha)}(\omega)/\omega$, computed from these spectral densities for the different local environments around the various BChl chromophores. The chromophores that are well coordinated by histidine side chains (BChls 1, 3, 4 and 6) generally have solvent reorganization energies of $\lambda_{his} \sim 15 \pm 2 \text{ cm}^{-1}$. Chromophore BChl7, with its more loosely coordinated histidine, has a reorganization energy of $\sim 20 \text{ cm}^{-1}$. Chromophore BChl5, which is bound to the backbone

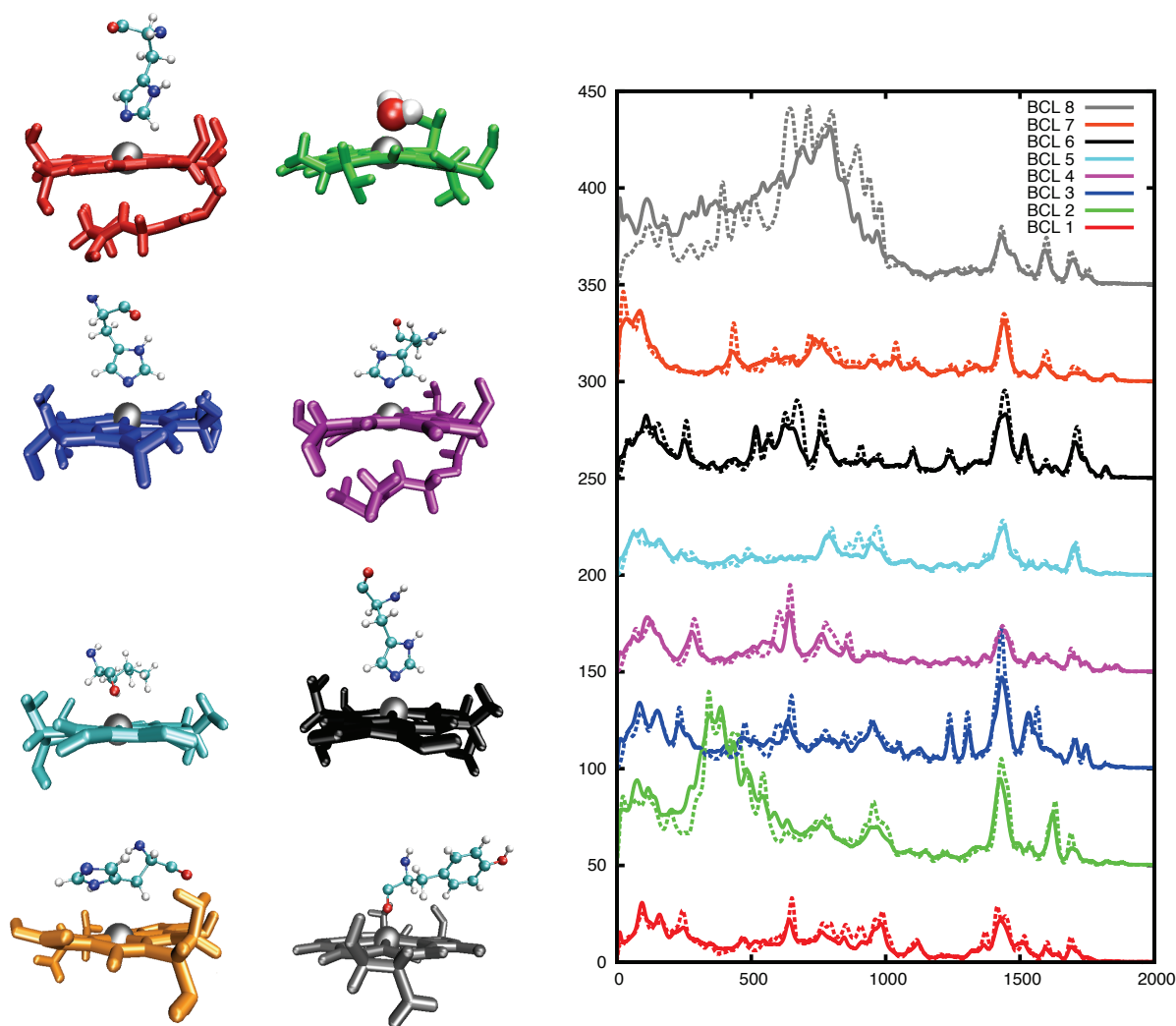


Figure 3: Left panel: Typical snapshot configuration of each of the BChls in an FMO monomer showing different local groups that coordinate the central magnesium of each porphyrin. The Mg atoms of BChls 1, 3, 4, and 6 are coordinated through the lone pairs on the N-atoms of different histidine side chains. Chromophore BChl7 is buried most deeply in the protein and its Mg atom is poorly coordinated by a histidine side chain. The Mg atoms of BChls 5 and 8 are coordinated through carbonyl (CO) groups at different points of the protein backbone. Finally BChl2 is in a pocket in the protein that is open to solvent and its central metal atom is typically coordinated by a water molecule. Right panel: BChl spectral densities calculated at 300 K (solid line) and 77 K (dashed line) using the partial charge difference coupling method. BChl spectral densities are averaged over the 3 monomers. Spectral densities are arranged in order from BChl 1 (bottom, red) to BChl 8 (top, gray) with an off set of 50 cm^{-1} on the y-axis for clarity.

and buried deep in the protein, has a reorganization energy of only $\sim 10 \text{ cm}^{-1}$. In significant contrast, the chromophores that are found in regions of considerable solvent accessibility, BChl2 and BChl8, have solvent reorganization energies *more than twice* those of the buried chromophores outlined above, with $\lambda_{\text{BChl2}} \sim 30 \text{ cm}^{-1}$ and $\lambda_{\text{BChl8}} \sim 40 \text{ cm}^{-1}$, respectively. These differences from chromophore to chromophore, in gross quantities that characterize chromophore - environment interactions, like solvent reorganization energies, actually result from detailed differences in the shapes of the spectral densities of the different chromophores as presented in Figure 3. For the FMO system, the low frequency structures in the different spectral densities are most important since the energy spacings and couplings between the chromophores, presented in Figure 2, are typically a few tens to about a hundred wavenumbers, and further the contributions to the local frictional force (see the solvent reorganization energy expression above) drop off like $1/\omega$.

The experimental nonlinear optical response results for the FMO system³ that prompted the recent interest in exploring the factors that influence long-lived quantum coherent dynamics of chromophore networks in biological systems involved the initial excitation of chromophore BChl1, which has strong electronic coupling to chromophore BChl2 (see Figure 2). The long-lived coherent quantum beats observed in the experimental signals are due to this strong excitonic coupling between these chromophores. The experimentally resolved dephasing dynamics of the initially excited coherent superposition was fit¹⁸ to a model that assumes that all chromophores have environments characterized by the same local response. The fitting model thus supposes that all chromophores interact with independent baths with the same lorentzian truncated ohmic, or Debye spectral density form, $J^{\text{exp}}(\omega) = 2\lambda\omega\tau_c/(1 + \omega^2\tau_c^2)$, with bath relaxation time $\tau_c = 50 \text{ fs}$ and solvent reorganization energy parameter $\lambda = 35 \text{ cm}^{-1}$.

The results of our detailed spectral density calculations presented in Figure 3 suggest that this model involving identical spectral densities for all the chromophores is an over-simplification. In fact, as outlined above, our calculations indicate that chromophore BChl2 is twice as strongly coupled to its environment compared to BChl1, so the dissipation from the initially excited coherent superposition of these two chromophores actually occurs asymmetrically, the features of the re-

laxation being captured, only on average, by the effective experimental chromophore independent spectral density model. In Figure 4 we compare these local spectral densities with the effective fitted model experimental spectral density.

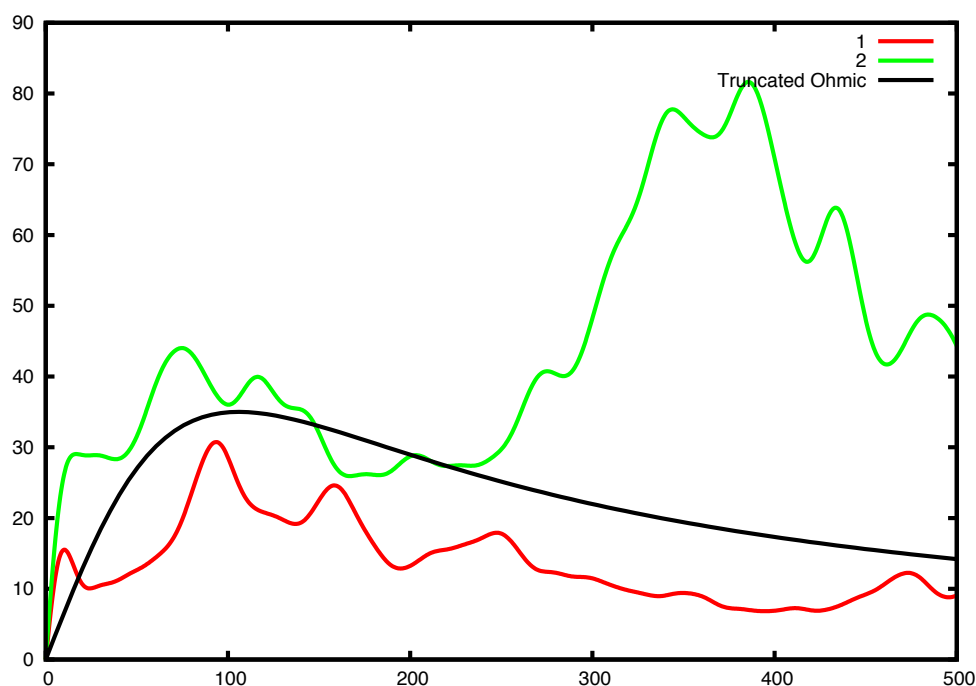


Figure 4: Comparison of computed spectral densities for chromophores BChl1 and BChl2. Also presented is the Debye spectral density that was used in the site-independent uniform spectral density model employed to fit the experimental signals.

It is interesting to note that our calculations suggest that this factor of two increase in environmental coupling as measured by local solvent reorganization energy of chromophore BChl2 over its immediate neighbors in the network (BChl1 and BChl3) arises partially as a result of the strong coupling to higher frequency modes of the hydrogen-bonded solvating water molecules that penetrate the region of the protein around chromophore BChl2 and polar residues in the protein pocket housing this chromophore (see below). This manifests itself in the double peaked structure of our computed spectral density for BChl2 shown in Figure 3 and highlighted in Figure 4. We see that the low frequency peak (less than 200 cm^{-1}), has roughly the same magnitude as those of the neighboring histidine bound chromophores (BChl1 and BChl3). The doubling of the solvent reorganization energy for chromophore BChl2, by comparison, results from the strong unique peak

in its spectral density between 300 and 500 cm^{-1} . Since this peak is about 3-4 times the magnitude of the lower frequency peak, and occurs at about 3-4 times the frequency it makes a contribution to the solvent reorganization energy that is comparable to that of the low frequency feature, effectively doubling the solvent reorganization energy of this chromophore compared to the others in this part of the excitation energy transfer network.

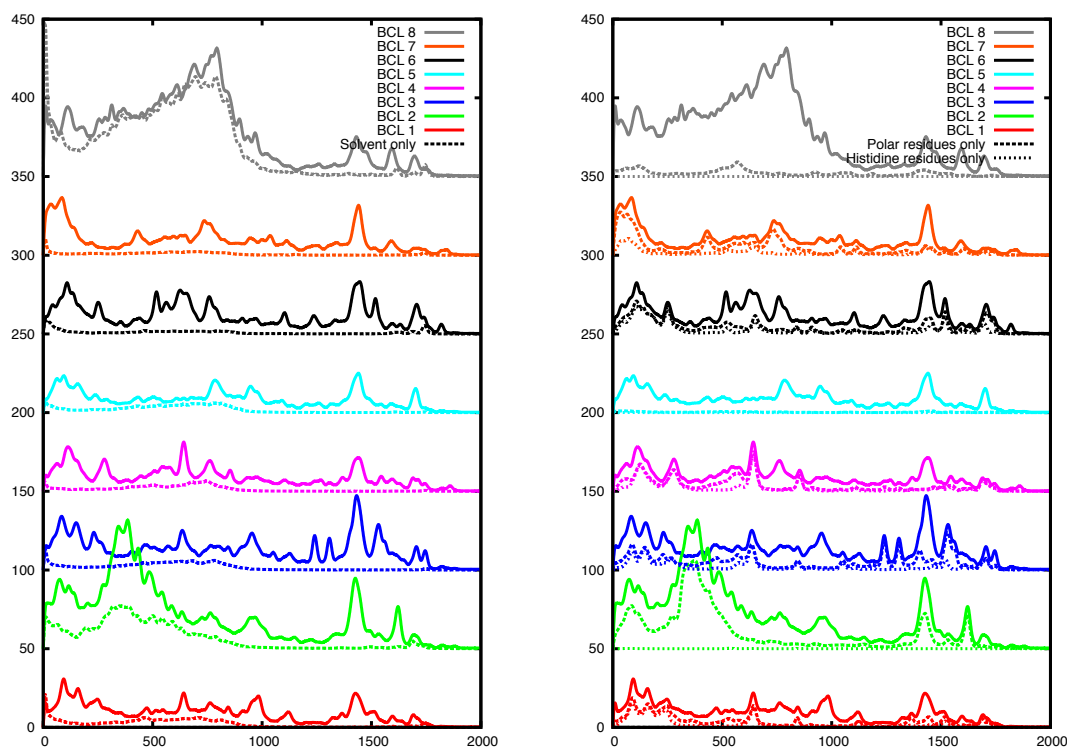


Figure 5: Analysis of component interactions contributing to site dependent spectral densities. Left panel: Compares the computed spectral densities including all interactions (solid curves) with calculations that include only of interactions with solvent molecules (dashed curves). Right panel: Compares computed spectral densities including all interactions (solid curves) with calculations that include only interactions with polar residues (long dashed curves), as well as computed results including only interactions with histidine residues (short dashes curves).

To begin to develop an understanding of what motions are involved in promoting excitation energy fluctuations of chromophore BChl2 in this frequency range, in Figure 5 we compare spectral densities computed by selectively switching on only certain parts of the environment and turning off the interactions with other components by setting their environmental partial charges to zero. Thus, in the left panel of Figure 5 we present the spectral densities of the different chromophores

Eva Rivera et al.

Influence of Site-Dependent Pigment- ...

calculated using only water solvent interactions to compute chromophore excitation energy fluctuations, while in the right panel we compare excitation energy contributions from environmental interactions computed using only partial charges from polar residues and histidines, respectively. From the left panel we see that only chromophores BChl2 and BChl8 have any appreciable spectral density contribution from fluctuations in the local water solvent environment. In fact, the spectral density of chromophore BChl8 is strongly dominated by contributions from water solvent fluctuations. Comparing the traces in the left and right panels for chromophore BChl2, however, suggests that the magnitude of the spectral density for this chromophore comes almost equally from fluctuations in the water solvent and fluctuations in the polar residues that line the protein pocket housing chromophore BChl2.

In order to explore the dynamical consequences of the local differences in spectral densities that we have found in the results outlined above we have performed a series of multi-state quantum dynamics calculations using the heterogeneous, site-dependent spectral density model hamiltonian obtained from our studies as well as variations on this model. We have treated this complex system dynamics using the general open system dissipative quantum dynamics methodology known as the partial linearized density matrix (PLDM) propagation approach that our group has developed and tested in a wide variety of non-perturbative, non-markovian, non-adiabatic model applications in recent work.^{25,26,30}

For completeness, in the Supporting Information we present results for the widely studied 7 chromophore model of FMO. As mentioned above, in our MD studies of the solvated trimer, each monomer unit includes the full complement of 8 BChl chromophores present in the *in vivo* system. It has been suggested⁷ that chromophore BChl8 plays the role of an “excitonic connection terminal” between the base plate of main light harvesting structure of the green sulfur bacteria, the chlorosome,⁴⁸ and the FMO “excitonic wire” that connects the base plate to the reaction center where charge separation is initiated. As we have observed in our simulations, chromophore BChl8 is highly solvent accessible and the fact that most ultrafast non-linear optical spectroscopy studies of the solvated FMO trimer alone (without the base plate and other support structures) show no

Eva Rivera et al.

Influence of Site-Dependent Pigment- ...

signals from this chromophore suggests that this most labile of chromophores is detached from the complex during sample preparation.⁷ Our calculations of the 7 BChl chromophore system employ the model system hamiltonian presented by Cho *et al.*⁴⁹ while we use the H_S model presented by Moix *et al.*⁸ for the 8 chromophore system. The bath and system-bath coupling terms used in these different models simply include, or leave out the eighth BChl chromophore bath, parameterized as detailed above.

In Figure 6 we present population dynamics results for the full 8 chromophore model computed at T=300K with various spectral density models. In particular we present results for both the full 8 chromophore site dependent spectral density model, and for a model in which we mutate the local environment around BChl2, by replacing its original spectral density with that of BChl1 and leaving all other chromophore environments unchanged. The upper panel considers the situation in which chromophore BChl1 is initially excited, mimicking the experimental initial conditions, but our simulation explores how the results are expected to be influenced when this excitation occurs in the presence of the additional eighth chromophore, and with this local mutation. We assume an initial non-equilibrium product density matrix with the initially uncoupled bath prepared in thermal equilibrium at T=300K, chromophore BChl1 in its excited state, and all other chromophores are initially unexcited. Below we will explore the influence of different initial excitations.

It is interesting to note that with the full 8 state site-dependent spectral density model initially excited in this way we see transient “up hill” excitation energy transfer from the initial coherent superposition state involving intermediate energy states BChl1 and BChl2 transferring population to the higher energy BChl8 state (see Figure 2 for details of the system hamiltonian parameters). The downward energy flow towards occupying the lower lying energy states BChl3 and BChl4 is driven by dissipation to the different chromophore environments. With this dynamics, the two states that are most strongly coupled to their environments in our state-dependent spectral density model (BChl2 and BChl8), are both significantly occupied and this seems to enhance the dephasing dynamics giving rapidly damped population oscillations of the BChl1 and BChl2 states. With the full site dependent model for initial excitation of BChl1 (solid curves in the upper panel of

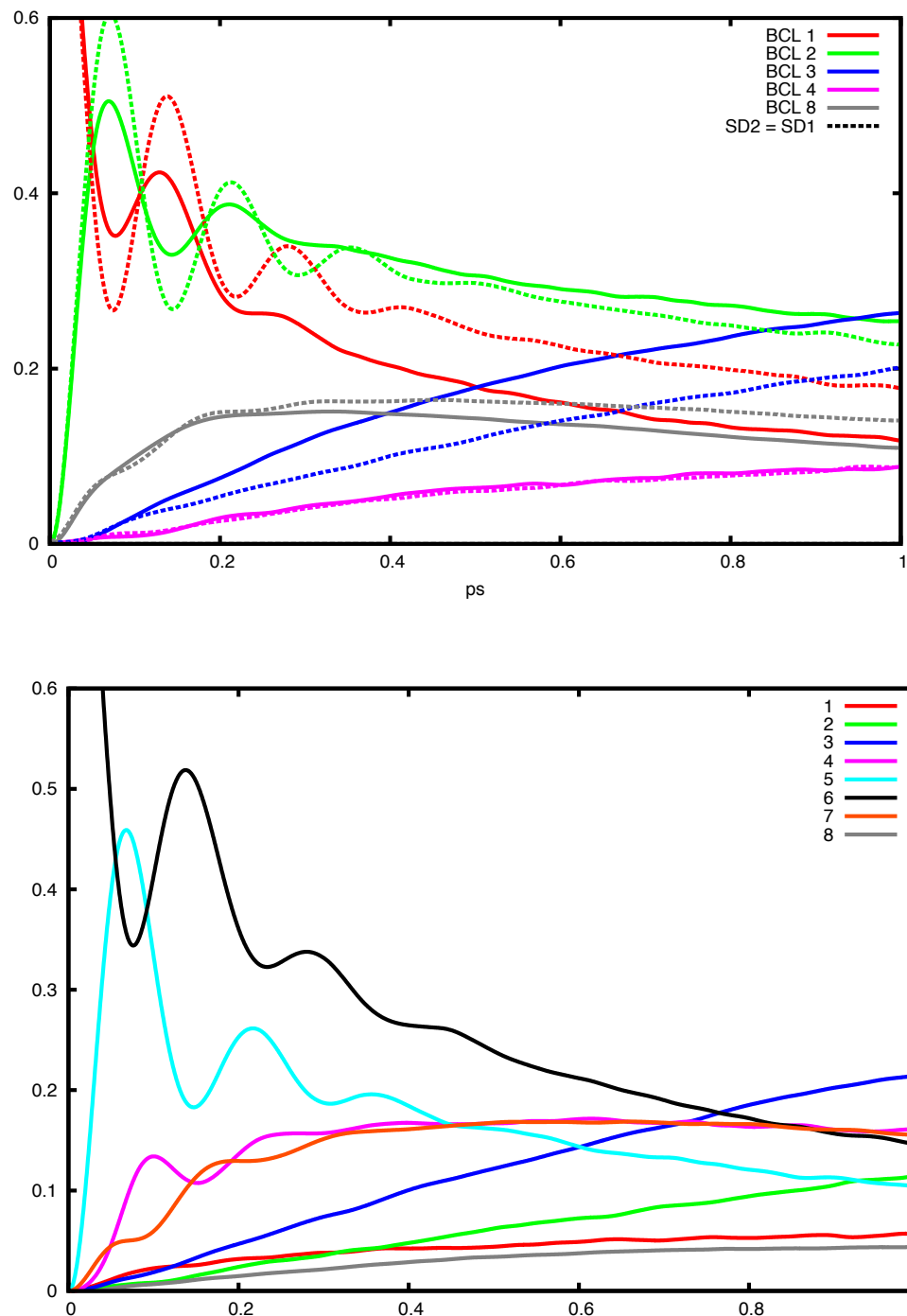


Figure 6: Population dynamics for eight state FMO model hamiltonian obtained from calculations with $T=300\text{K}$. Solid curves gives results computed using the calculated state dependent spectral density model. Dashed curves give populations obtained using a model hamiltonian in which the computed site-dependent spectral density of chromophore BChl2 has been replaced by that of chromophore BChl1, thus modeling a local mutation of the protein structure around chromophore BChl2. Upper panel gives results with chromophore BChl1 initially excited. Lower panel gives results for the full un-mutated site dependent-spectral model only, but chromophore BChl6 is initially excited.

Figure 6) we see damped coherent population oscillations out to about 250 fs, comparable to the decoherence times observed in the experimental results under these conditions.¹ However, the population dynamics we find with the “mutant” spectral density model in which we replace the strongly dissipative environment around chromophore BChl2 by the same weakly interacting environment as around BChl1 (dashed curves in the upper panel of Figure 6) gives a decoherence time of more than 500 fs, significantly longer than observed in the experiments under these conditions, pointing to the importance of the local heterogeneity of dissipation captured by our full site dependent spectral density model. We see that the effect of this longer lived coherent dynamics with the mutant spectral density is to significantly slow the population transfer to chromophore BChl3 that funnels excitation energy to the reaction center.

In the lower panel of Figure 6 we present our population dynamics results computed for the full 8 chromophore site-dependent spectral density model, only here we explore the evolution of the excitation along a different pathway through the network starting with chromophore BChl6 initially excited. Due to the connectivity of the network, the dynamics resulting from this initial excitation involves only chromophores that are buried deep within the protein that are protected from the strongly dissipative environment of the water solvent. From Figure 2 we see that the chromophores BChl6-BChl5 and BChl4-BChl7 participate in a completely independent energy transfer pathway from the “ring-road” route of the FMO excitation energy transfer network, explored in the calculations outlined above, involving BChl8-BChl1-BChl2-BChl3, which makes its way around the outer regions of the complex, encountering significant dissipative solvent interactions along the way particularly involving BChl8 and BChl2. From the parameters summarized in Figure 2, computed for our full simulations of the FMO trimer system, we see that for the “through-town” route involving the chromophore dimers BChl6-BChl5 and BChl4-BChl7, all the site-dependent solvent reorganization energy parameters are *on average about half the largest magnitudes* of those of chromophores BChl8-BChl1-BChl2-BChl3 in the ring-road route. The through-town route chromophores are arranged as a pair of electronically coupled “dimers” with the BChl6-BChl5 dimer having an excitation energy difference of 85 cm^{-1} and interchromophore electronic coupling of 89

Eva Rivera et al.

Influence of Site-Dependent Pigment- ...

cm⁻¹, while the BChl4-BChl7 dimer excitation energy difference is 90 cm⁻¹ with dimer electronic coupling of -64 cm⁻¹. These dimers in the through-town pathway thus have similar magnitude parameters that govern the quantum coherent population oscillations to the BChl1-BChl2 dimer in the ring-road pathway where the excitation energy gap is 80 cm⁻¹, with dimer electronic coupling of -98 cm⁻¹. From the lower panel of Figure 6 we see that the initially excited coherent beating of the BChl6-BChl5 dimer transfers to the BChl4-BChl7 dimer as excitation energy moves through this region of the chromophore network. As noted above, because these chromophores of the through-town route that are buried in protein in the FMO trimer interact weakly with their local protein only environment, where as various chromophores on the ring-road route experience strong solvent dissipation, the oscillations in populations of the two chromophore dimers, BChl6-BChl5 and BChl4-BChl7, on the buried through-town route show significantly longer lived coherence, with oscillations persisting out beyond 500 fs in the T=300K results presented in the bottom panel of Figure 6, mimicking the mutant results discussed above, and in sharp contrast to the over-damped oscillations of the solid curves in the upper panel that show rapid decoherence in about 250 fs for the BChl1-BChl2 dimer along the “wild-type” ring-road route. This significant difference in dephasing rates between these two electronically disconnected routes through this complex should be observable experimentally providing a stringent test of the predictions of our calculations that suggest that there should be considerable differences in relaxation processes along these different energy transfer pathways in the FMO trimer system. In the Supporting Information we present population dynamics results for initially exciting chromophore BChl5 in the FMO trimer, which calculations suggest, is possibly in a slightly clearer window of excitation wavelength and we again see evidence of persistent strong coherent beating and slower energy transfer on this through-town route.

Conclusion

In this communication we have demonstrated that the population dynamics in typical parameter ranges for the solvated FMO trimer complex is expected to be sensitive to differences in the details of the local environmental interactions of the various chromophores as characterized by realistically parameterized site-dependent spectral densities. Using classical GS MD simulations and a point charge difference model to describe environmentally induced excitation energy fluctuations we find that the spectral densities characterizing the different chromophore environments vary significantly from chromophores near the protein-solvent interface, where strong interactions with water molecules can cause rapid energy relaxation and dephasing, to chromophores buried deep in the protein that can experience environmental interactions that are typically two to three times weaker resulting in slower relaxation from these parts of the chromophore network.

Quantum dynamics calculations, using the computed site dependent spectral densities, suggest that initially exciting these energy transfer networks in different ways should pick out distinct pathways through the chromophore complex that may be characterized by the different types of chromophore - environment interactions depending on if the pathway involves only chromophores buried deep in the protein scaffold, or if the pathway includes chromophores that are in interfacial regions where stronger interactions with solvent can have a profound influence on network energy dissipation.

These findings point to an interesting design concept that seems to be at play at least in the FMO excitonic wire pigment-protein complex. This design principle suggests that the fastest pathway through an excitation energy transfer network should take advantage of differences in local relaxation processes to most efficiently move the excitation energy downhill towards the reaction center. Our calculations indicate that such optimal energy transfer pathways should probably involve chromophores at the interface of the complex with its solvent environment rather than moving energy through chromophores buried in the protein as such protein protected chromophores necessarily dissipate energy less efficiently and so along such pathways energy transfer takes longer to relax down hill. If, rather than energy transfer efficiency, we were interested in taking advantage of

Eva Rivera et al.

Influence of Site-Dependent Pigment- ...

longer lived quantum coherent dynamics in these systems,¹⁹ using pathways that take excitation through the protein, and effectively provide coherent insulation against solvent “short circuiting” of quantum coherent information may provide an interesting strategy to extend the life time of coherent superposition states in complex biological and polymer systems.

Our calculations suggest that if different pathways through biological chromophore networks can be selectively excited, the differences in local relaxation processes should be observable using dephasing time measurements. Another way that these differences might be explored is by changing the dissipative characteristics of local environments around different chromophores. Our studies reveal that local protein mutation, which we mimic by modifying spectral densities, can profoundly influence relaxation processes in these chromophore networks. Alternatively, opening different regions of the protein up to access by solvent should also significantly influence network relaxation. In the FMO trimer, for example, the through-town pathway is buried by the protein-protein interface between the monomers. In the FMO monomer, on the other hand, chromophores in this pathway should be exposed to solvent, opening new dissipation possibilities. The dephasing measurements on different pathways should offer a useful probe of chromophore - solvent accessibility in these different structures.

The notion of employing local environmental fluctuations as a design element for controlling energy transport in nano structured systems builds on the ideas of stochastic resonance and environmentally, or noise assisted quantum transport phenomena^{50–54} in which the energy transfer rate through such chromophore network systems is observed to be optimized by exploiting processes analogous to Kramers turnover like effects observed in barrier crossing phenomena.³⁴ Our studies suggest that these types of processes might be used to implement local dynamical control of energy transport pathways and mechanisms.

Acknowledgement

We gratefully acknowledge support for this research from the U.S. National Science Foundation under grant CHE-0911635 and support from Science Foundation Ireland under grant number 10/IN.1/I3033. DFC acknowledges the support of his Stokes Professorship in Nanobiophysics from Science Foundation Ireland. MM acknowledges funding from the EU Marie Curie Fellowship programme *FP7-PEOPLE-2011-IOF* (contract number PIOF-GA-2011-299345), as well as the European Science Foundation (ESF- Ψ_k) for the activity titled “Advanced Concepts in *ab-initio* Simulations of Materials” (Grant 4294), and the UCD Atlantic Center for Atomistic Modeling (ACAM) for support of short exchange visits to Dublin that initiated this research. We also acknowledge useful discussions with Dr. Pengfei Huo and Prof. Pietro Ballone, as well as grants of supercomputer resources from Boston University’s Office of Information Technology and Scientific Computing and Visualization and the Irish Center for High End Computing (ICHEC).

Supporting Information Available

Simulation details of solvated FMO trimer molecular mechanics calculations; Bacteriochlorophyll ground state partial charge model; Statistical convergence study of calculated spectral densities; Demonstration of unphysical temperature dependent spectral densities computed by processing classical excitation energy correlation functions with quantum expression; Study of population dynamics of excited seven BChl chromophore FMO model and Population dynamics after exciting eight state FMO model initially to BChl5. This information is available free of charge via the Internet at <http://pubs.acs.org>.

References

- 1 Panitchayangkoona, G.; Hayes, D.; Fransted, K. A.; Caram, J. R.; Harel, E.; Wen, J.; Blankenship, R.E. and Engel, G.S. Long-Lived Quantum Coherence in Photosynthetic Complexes at

Eva Rivera et al.

Influence of Site-Dependent Pigment- ...

- Physiological Temperature. *Proc. Natl. Acad. Sci.* **2010**, *107*, 12766-12770.
- 2 Collini, E.; Wong, C.Y.; Wilk, K.E.; Curmi, P.M.G.; Brumer, P. and Scholes, G.D. Coherently Wired Light-Harvesting in Photosynthetic Marine Algae at Ambient Temperature. *Nature* **2010**, *463*, 644-648.
- 3 Engel, G.S.; Calhoun, T.R.; Read, E.L.; Ahn, T.-K.; Mancal, T.; Cheng, Y.-C.; Blankenship, R.E. and Fleming, G.R. Evidence for Wavelike Energy Transfer Through Quantum Coherence in Photosynthetic Systems. *Nature* **2007**, *446*, 782-786.
- 4 Lee, H.; Cheng, Y.-C. and Fleming, G.R. Coherence Dynamics in Photosynthesis: Protein Protection of Excitonic Coherence. *Science* **2007**, *316*, 1462-1465.
- 5 Ben-Shem, A.; Frolow, F.; Nelson, N. Evolution of Photosystem I D From Symmetry Through Pseudosymmetry to Asymmetry. *FEBS Lett.* **2004**, *564*, 274-280.
- 6 Tronrud, D.E.; Wen, J.; Gay, L.; Blankenship, R. E. The Structural Basis for the Difference in Absorbance Spectra for the FMO Antenna Protein from Various Green Sulfur Bacteria. *Photosynth. Res.* **2009**, *100*, 79-87.
- 7 Schmidt am Busch, M.; Muh, F.; Madjet, M. and Renger, T. The Eighth Bacteriochlorophyll Completes the Excitation Energy Funnel in the FMO Protein. *J. Phys. Chem. Lett.* **2011**, *2*, 93.
- 8 Moix, J.; Wu, J.; Huo, P.; Coker, D.F. and Cao, J. Efficient Energy Transfer in Light-Harvesting Systems, III: The Influence of the Eighth Bacteriochlorophyll on the Dynamics and Efficiency in FMO. *J. Phys. Chem. Lett.* **2011**, *2*, 3045-3052.
- 9 Jang, S.; Newton, M.D. and Silbey, R.J. Multichromophoric Förster Resonance Energy Transfer. *Phys. Rev. Lett.* **2004**, *92*, 218301/1-218301/4.
- 10 Jang, S.; Newton, M.D. and Silbey, R.J. Multichromophoric Förster Resonance Energy Transfer from B800 to B850 in the Light Harvesting Complex 2: Evidence for Subtle Energetic Optimization by Purple Bacteria. *J. Phys. Chem. B* **2007**, *111*, 6807-6814.

Eva Rivera et al.

Influence of Site-Dependent Pigment- ...

- 11 Heijs, D.J.; Malyshev, V.A. and Knoester, J. Decoherence of Excitons in Multichromophore Systems: Thermal Line Broadening and Destruction of Superradiant Emission. *Phys. Rev. Lett.* **2005**, *95*, 177402/1-177402/4.
- 12 Schröder, M.; Kleinekathöfer, U. and Schreiber, M. Calculation of Absorption Spectra for Light-Harvesting Systems Using Non-Markovian Approaches as well as Modified Redfield Theory. *J. Chem. Phys.* **2006**, *124*, 084903/1-084903/14.
- 13 Palmieri, B.; Abramavicius, D. and Mukamel, S. Lindblad Equations for Strongly Coupled Populations and Coherences in Photosynthetic Complexes. *J. Chem. Phys.* **2009**, *130*, 204512/1-204512/10.
- 14 Olaya-Castro, A.; Fan-Lee, C.; Fassioli-Olsen, F. and Johnson, N.F. Efficiency of Energy Transfer in a Light-Harvesting System Under Quantum Coherence. *Phys. Rev. B* **2008**, *78*, 085115/1-085115/7.
- 15 Cheng, Y. C. and Silbey, R. J. Markovian Approximation in the Relaxation of Open Quantum Systems. *J. Phys. Chem. B.* **2005**, *109*, 21399-21405.
- 16 Ishizaki, A. and Fleming, G.R. On the Adequacy of the Redfield Equation and Related Approaches to the Study of Quantum Dynamics in Electronic Energy Transfer. *J. Chem. Phys.* **2009**, *130*, 234110/1-234110/9.
- 17 Ishizaki, A. and Fleming, G.R. Unified Treatment of Quantum Coherent and Incoherent Hopping Dynamics in Electronic Energy Transfer: Reduced Hierarchy Equation Approach. *J. Chem. Phys.* **2009**, *130*, 234111/1-234111/10.
- 18 Ishizaki, A. and Fleming, G.R. Theoretical Examination of Quantum Coherence in a Photosynthetic System at Physiological Temperature. *Proc. Natl. Acad. Sci.* **2009**, *106*, 17255-17260.
- 19 Sarovar, M.; Ishizaki, A.; Fleming, G.R. and Whaley, K.B. Quantum Entanglement in Photosynthetic Light-Harvesting Complexes. *Nature Physics* **2010**, *6*, 462-467.

Eva Rivera et al.

Influence of Site-Dependent Pigment- ...

- 20 Wu, J.; Liu, F.; Shen, Y.; Cao, J. and Silbey, R.J. Efficient Energy Transfer in Light-Harvesting Systems, I: Optimal Temperature, Reorganization Energy, and Spatial-Temporal Correlations. *New J. Phys.* **2010**, *12*, 105012/1-105012/17.
- 21 Tao, G. and Miller, W.H. Semiclassical Description of Electronic Excitation Population Transfer in a Model Photosynthetic system. *J. Phys. Chem. Lett.* **2010**, *1*, 891-894.
- 22 Zhang, W. M.; Meier, T. ; Chernyak, V. and Mukamel, S. Exciton-Migration and Three-Pulse Femtosecond Optical Spectroscopies of Photosynthetic Antenna Complexes. *J. Chem. Phys.* **1998**, *108*, 7763-7714.
- 23 Yang, M. and Fleming, G.R. Influence of Phonons on Exciton Transfer Dynamics: Comparison of the Redfield, Förster, and Modified Redfield Equations. *Chem. Phys.* **2002**, *282*, 163-180.
- 24 Pomyalov, A. and Tannor, D. The Non-Markovian Quantum Master Equation in the Collective-Mode Representation: Application to Barrier Crossing in the Intermediate Friction Regime. *J. Chem. Phys.* **2005**, *123*, 204111/1-204111/11.
- 25 Huo, P. and Coker, D.F. Partial Linearized Density Matrix Dynamics for Dissipative, Non-Adiabatic Quantum Evolution. *J. Chem. Phys.* **2011** *135*, 201101.
- 26 Huo, P. and Coker D.F. Consistent Schemes for Non-Adiabatic Dynamics Derived from Partial Linearized Density Matrix Propagation. *J. Chem. Phys.* **2012** *137*, 22A535.
- 27 Dunkel, E.R.; Bonella, S. and Coker, D.F. Iterative Linearized Approach to Nonadiabatic Dynamics. *J. Chem. Phys.* **2008**, *129*, 114106/1-114106/15.
- 28 Bonella, S. and Coker, D.F. LAND-map, a Linearized Approach to Non-Adiabatic Dynamics using the Mapping Formalism. *J. Chem. Phys.* **2005**, *122*, 194102/1-194102/13.
- 29 Bonella, S.; Montemayor, D. and Coker, D.F. Linearized Path Integral Approach for Calculating Nonadiabatic Time Correlation Functions. *Proc. Natl. Acad. Sci.* **2005**, *102*, 6715-6719.

Eva Rivera et al.

Influence of Site-Dependent Pigment- ...

- 30 Huo, P. and Coker, D.F. Semi-Classical Path Integral Nonadiabatic Dynamics: A Partial Linearized Classical Mapping Hamiltonian Approach. *Mol. Phys.* **2012** *110*, 1035-1052.
- 31 Huo, P.; Bonella, S.; Chen, L. and Coker, D.F. Linearized Approximations for Condensed Phase Non-Adiabatic Dynamics: Multi-Layered Baths and Brownian Dynamics Implementation. *Chem. Phys.* **2010**, *370*, 87-97.
- 32 Huo, P. and Coker, D.F. Iterative Linearized Density Matrix Propagation for Modeling Coherent Excitation Energy Transfer in Photosynthetic Light Harvesting. *J. Chem. Phys.* **2010** *133*, 184108.
- 33 Leggett, A.J.; Chakravarty, S.; Dorsey, A.T.; Fisher, M.P.A. and Garg, A. Dynamics of the dissipative two-state system *Rev. Mod. Phys.* **1987** *59*, 1.
- 34 Nitzan, A. Chemical Dynamics in Condensed Phases (Oxford University Press, Oxford) **2006**.
- 35 Valleau, S.; Eisfeld, A. and Aspuru-Guzik, A. On the Alternatives for Bath Correlators and Spectral Densities from Mixed Quantum-Classical Simulations. *J. Chem. Phys.* **2012**, *137*, 224103.
- 36 Shim, S.; Rebentrost, P.; Valleau, S.; and Aspuru-Guzik, A. Atomistic Study of the Long-Lived Quantum Coherences in the Fenna-Matthews-Olsen Complex. *Biophys. J.* **2012**, *102* 649-660.
- 37 Renger, T.; Klinger, A.; Steinecker, F.; Schmidt am Busch, M.; Numata, J. and Mueh, F. Normal Mode Analysis of the Spectral Density of the Fenna-Matthews-Olsen Light Harvesting Protein: How the Protein Dissipates the Excess Energy of Excitons. *J. Phys. Chem. B.* **2012**, *116*, 3094935.
- 38 Raszewski, G.; Saenger, W. and Renger, T. Light Harvesting in Photosystem II Core Complexes is Limited by the Transfer to the Trap: Can the Core Complex Turn Into a Photoprotective Mode? *J. Am. Chem. Soc.* **2008**, *130*, 4431.

Eva Rivera et al.

Influence of Site-Dependent Pigment- ...

- 39 Madjet, M.E.; Abdurahman, A. and Renger, T. Intermolecular Coulomb Couplings From *Ab Initio* Electrostatic Potentials: Application to Optical Transitions of Strongly Coupled Pigments in Photosynthetic Antennae and Reaction Centers. *J. Phys. Chem. B.* **2006**, *110*, 17268-17281.
- 40 Jing, Y.; Zheng, R.; Li, H.-X. and Shi, Q. Theoretical Study of the Electronic-Vibrational Coupling in the Q(y) States of the Photosynthetic Reaction Center in Purple Bacteria. *J. Phys. Chem. B.* **2012**, *116*, 1164-1171.
- 41 Damjanovic, A.; Kosztin, I.; Kleinekathofer, U. and Schulten, K. Excitons in a Photosynthetic Light-Harvesting System: A Combined Molecular Dynamics, Quantum Chemistry, and Polariton Model Study. *Phys. Rev. E.* **2002**, *65*, 031919.
- 42 Olbrich, C. and Kleinekathoefer, U. Time-Dependent Atomistic View of the Electronic Relaxation in Light-Harvesting System II. *J. Phys. Chem. B.* **2010**, *114*, 12427-12437.
- 43 Olbrich, C.; Jansen, T. L. C.; Liebers, J.; Aghtar, M.; Struempfer, J.; Schulten, K.; Knoester, J. and Kleinekathoefer, U. From Atomistic Modeling to Excitation Transfer and Two-Dimensional Spectra of the FMO Light-Harvesting Complex. *J. Phys. Chem. B.* **2011**, *115*, 8609-8621.
- 44 Olbrich, C.; Struempfer, J.; Schulten, K. and Kleinekathoefer, U. Quest for Spatially Correlated Fluctuations in the FMO Light-Harvesting Complex. *J. Phys. Chem. B.* **2011**, *115*, 758-764.
- 45 Olbrich, C.; Struempfer, J.; Schulten, K. and Kleinekathoefer, U. Theory and Simulation of the Environmental Effects on FMO Electronic Transitions. *J. Phys. Chem. Lett.* **2011**, *2*, 1771-1776.
- 46 Kim, H.W.; Kelly, A.; Park, J.W. and Rhee, Y.M. All-Atom Semiclassical Dynamics Study of Quantum Coherence in Photosynthetic Fenna-Matthews-Olson Complex. *J. Am. Chem. Soc.* **2012**, *134*, 11640-11651.

Eva Rivera et al.

Influence of Site-Dependent Pigment- ...

- 47 Zwier, M.; Shorb, J. and Krueger, B.J. Hybrid Molecular Dynamics-Quantum Mechanics Simulations of Solute Spectral Properties in the Condensed Phase: Evaluation of Simulation Parameters. *J. Comput. Chem.* **2007**, *28*, 1572-1581.
- 48 Fujita, T.; Brookes, J.C.; Semion, S.K. and Aspuru-Guzik, A. Memory-Assisted Exciton Diffusion in the Chlorosome Light-Harvesting Antenna of Green Sulfur Bacteria *J. Phys. Chem. Letts* **2012**, *3*, 2537.
- 49 Cho, M.; Vaswani, H.M.; Brixner, T.; Stenger, J. and Fleming, G. R. Exciton Analysis in 2D Electronic Spectroscopy *J. Phys. Chem. B.* **2005**, *109*, 10542.
- 50 Rebentrost, P.; Mohseni, M. and Aspuru-Guzik A. Role of Quantum Coherence and Environmental Fluctuations in Chromophoric Energy Transport *J. Phys. Chem. B* **2009**, *113*, 9942; Rebentrost, P.; Mohseni, M.; Kassal, I.; Lloyd, S. and Aspuru-Guzik, A. Environment-assisted Quantum Transport. *New. J. Phys.* **2009**, *11*, 033003.
- 51 Rebentrost, P. and Aspuru-Guzik, A. Communication: Exciton-Phonon Information Flow in the Energy Transfer Process of Photosynthetic Complexes *J. Chem. Phys.* **2011**, *134*, 101103.
- 52 Caruso, F; Chin, A.W.; Datta, A.; Huelga, S.F. and Plenio, M.B. Highly Efficient Excitation Energy Transfer in Light-Harvesting Complexes: The Fundamental Role of Noise-Assisted Transport *J. Chem. Phys.* **2009**, *131*, 105106; Plenio, M.B. and Huelga, S.F. Dephasing-Assisted Transport: Quantum Networks and Biomolecules *New J. Phys.* **2008**, *10*, 113019; Caruso, F; Chin, A.W.; Datta, A.; Huelga S.F. and Plenio, M.B. Entanglement and Entangling Power of the Dynamics in Light-Harvesting Complexes *Phys. Rev. A* **2010**, *81*, 062346; Chin, A.W.; Datta, A.; Caruso, F; Huelga, S.F. and Plenio, M.B. Noise-Assisted Energy Transfer in Quantum Networks and Light-Harvesting Complexes *New J. Phys* **2010**, *12*, 065002.
- 53 Cao, J. and Silbey, R.J. Optimization of Exciton Trapping in Energy Transfer Processes. *J. Phys. Chem. A.* **2009**, *113*, 13826-13838.

Eva Rivera et al.

Influence of Site-Dependent Pigment- ...

- 54 Huo, P. and Coker, D.F. Theoretical Study of Coherent Excitation Energy Transfer in Cryptophyte Phycocyanin 645 at Physiological Temperature J. Phys. Chem. Lett. **2011**, 2, 825.

